

Carrier recombination mechanisms and efficiency droop in GaInN/GaN light-emitting diodes

Qi Dai,¹ Qifeng Shan,¹ Jing Wang,¹ Sameer Chhajed,¹ Jaehee Cho,¹ E. Fred Schubert,^{1,a)} Mary H. Crawford,² Daniel D. Koleske,² Min-Ho Kim,³ and Yongjo Park³

¹Department of Physics, Applied Physics and Astronomy and Department of Electrical, Computer, and Systems Engineering, Rensselaer Polytechnic Institute, Troy, New York 12180, USA

²Sandia National Laboratories, Albuquerque, New Mexico 87185, USA

³R&D Institute, Samsung LED, Suwon 443-743, Republic of Korea

(Received 18 August 2010; accepted 7 September 2010; published online 30 September 2010)

We model the carrier recombination mechanisms in GaInN/GaN light-emitting diodes as $R = An + Bn^2 + Cn^3 + f(n)$, where $f(n)$ represents carrier leakage out of the active region. The term $f(n)$ is expanded into a power series and shown to have higher-than-third-order contributions to the recombination. The total third-order nonradiative coefficient (which may include an $f(n)$ leakage contribution and an Auger contribution) is found to be $8 \times 10^{-29} \text{ cm}^6 \text{ s}^{-1}$. Comparison of the theoretical $ABC + f(n)$ model with experimental data shows that a good fit requires the inclusion of the $f(n)$ term. © 2010 American Institute of Physics. [doi:10.1063/1.3493654]

The “efficiency droop” in GaInN/GaN light-emitting diodes (LEDs) is the gradual decrease of efficiency as the injection current density surpasses a value that typically ranges between 0.1 and 10 A/cm².¹ In order to comprehensively investigate the efficiency droop, we analyze the carrier recombination inside quantum wells (QWs) by means of $An + Bn^2 + Cn^3$ (ABC model), and carrier recombination outside of QWs by means of $f(n)$ (carrier leakage),^{1–3} where n is carrier concentration. A , B , and C represent the Shockley–Read–Hall (SRH), radiative, and Auger coefficient, respectively. The leakage of carriers out of QWs was found for GaInN/GaN LEDs under optical excitation.⁴ Droop-causing mechanisms based on recombination outside of QWs include lack of electron capture into QWs, electron escape from QWs, the electron-attracting properties of the spacer-electron blocking layer (EBL) interface, the p-type doping properties of EBL, and the asymmetry in electron and hole transport properties in GaN,^{1–7} all of which can lead to carrier leakage out of the active region. Droop-causing mechanisms based on recombination inside QWs (without leakage)⁹ include carrier delocalization⁸ and Auger recombination.⁹ We show that the comparison of the $ABC + f(n)$ model with experimental data provides useful insights into the efficiency droop and suggests that $f(n)$ depends on the device structure and can have second, third, and higher-order contributions.

Experimental studies are performed on two types of typical GaInN/GaN multi-quantum well (MQW) LEDs grown on *c*-plane sapphire substrates by metal-organic vapor-phase epitaxy. The first type is denoted as LED-1; it consists of a five-period GaInN/GaN MQW active region that emits at approximately 465 nm with 3 nm QWs and 12 nm quantum barriers. The chip area is $300 \times 300 \mu\text{m}^2$. The second type of LED is a series denoted as LED-S1, LED-S2, and LED-S5 having 1 QW, 2 QWs, and 5 QWs, respectively. Each QW is 2.3 nm wide separated by 7.5 nm barriers. The peak wavelengths at 25 mA forward current are 431 nm, 436 nm, and 444 nm, respectively. LEDs with three different chip areas, $200 \times 200 \mu\text{m}^2$, $300 \times 300 \mu\text{m}^2$, and $1 \times 1 \text{ mm}^2$, are fabricated. The unencapsulated devices are tested under

pulsed mode from 10 μA to 100 mA with 500 μs pulse duration and 1% duty cycle. Junction heating is not anticipated to be a factor under the employed pulsed condition. This is verified by the fact that lower duty cycles and shorter pulses do not yield different results.

For the GaInN/GaN LEDs, we write the recombination rate as $R = An + Bn^2 + Cn^3 + f(n)$, and expand the leakage term $f(n)$ into a power series (Taylor series), that is $f(n) = \alpha n + \beta n^2 + \gamma n^3 + \delta n^4 + \epsilon n^5 + \dots$. The recombination rate can then be written as follows:

$$R = A'n + B'n^2 + C'n^3 + D'n^4 + E'n^5 + \dots, \quad (1)$$

where $A' = A + \alpha$, $B' = B + \beta$, $C' = C + \gamma$, $D' = \delta$, and $E' = \epsilon$.

As the injection current increases, an increasing number of higher-order terms come into action; under low and moderate electrical injection, when the combination of the first three terms is sufficient, current (I) and collected light output power (LOP) can be expressed as follows:

$$I = \eta_1(A'n + B'n^2 + C'n^3), \text{ and } LOP = \eta_2 Bn^2, \quad (2)$$

where $\eta_1 (= qV_{\text{active}})$ is a constant given by the product of elementary charge q and effective active region volume V_{active} ; η_2 is another constant. We define the following:

$$x = \sqrt{LOP} = \sqrt{B\eta_2}n, \text{ and} \quad (3a)$$

$$y = \frac{LOP}{I} = \frac{B\eta_2}{\eta_1} \frac{1}{A'/n + B' + C'n}, \quad (3b)$$

where x is a measure of carrier concentration ($x \propto n$) and y is a measure of external quantum efficiency (EQE) ($y \propto \text{EQE}$), respectively. The maximum EQE is reached when $d\text{EQE}/dn = 0$, or $dy/dn = 0$, or $dy/dx = 0$. Using the condition $dy/dn = 0$ and Eq. (3) yields the following:

$$n_0 = \sqrt{A'/C'}, \quad x_0 = \sqrt{B\eta_2} \sqrt{A'/C'}, \text{ and} \\ y_0 = \frac{B\eta_2}{\eta_1} \frac{1}{B' + 2\sqrt{A'C'}}. \quad (4)$$

where n_0 , x_0 , and y_0 are values at the efficiency-peak point. Forming the ratio of y to y_0 by using Eqs. (3) and (4), one obtains the following:

^{a)}Electronic mail: efschubert@rpi.edu.

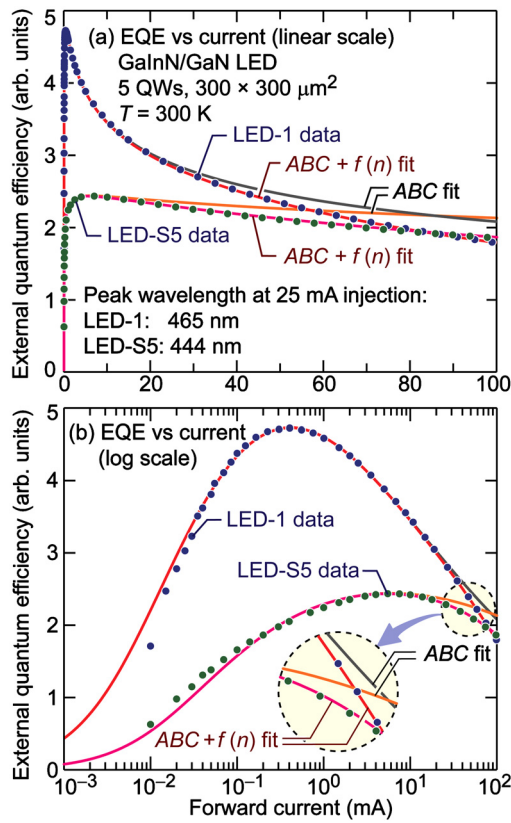


FIG. 1. (Color online) External quantum efficiency vs current and theoretical ABC model and $ABC+f(n)$ model fits (a) on linear and (b) log scale. Whereas the $ABC+f(n)$ model gives an excellent fit, the ABC model deviates from experimental results at high currents.

$$\frac{y}{y_0} = \frac{B'/\sqrt{A'C'} + 2}{B'/\sqrt{A'C'} + (x_0/x + x/x_0)} = \frac{P+2}{P + (x_0/x + x/x_0)}, \quad (5)$$

where we use the dimensionless parameter $P=B'/\sqrt{A'C'}$ that can be adjusted to fit experimental data. Equation (5) describes a family of curves, in the (x,y) diagram, all of which go through the origin $(0,0)$ and the peak (x_0,y_0) . For each experimental EQE versus I curve, x/x_0 and y/y_0 are known; P can be obtained by a least-square fitting of Eq. (5) to the experimental data. The variables x and y are related to current and efficiency by $I=x^2/y$ and $\text{EQE} \propto y$, respectively.

Figure 1 shows the EQE as a function of forward current and associated fitting curves for the two types of samples. Because we use the experimental values for x_0 and y_0 , the experimental and theoretical curves have the same efficiency-peak values and efficiency-peak current. For both samples, reasonable fits can only be obtained at low currents. However, the fits deviate from experimental data for a wide range of currents beyond the peak-efficiency points. A good fit is not attainable by adjusting the ABC -model parameters without including $f(n)$. Alternatively, excellent fits can be obtained by including higher order terms ($n^{>3}$), which is also shown in Fig. 1 as $ABC+f(n)$ model fitting. At 100 mA (111 A/cm^2), the higher-than-third-order terms contribute 14% and 13% to the total recombination rates of the LED-1 and LED-S5, respectively. Note that the higher-than-third-order terms are just part of the total leakage term $f(n)$.

To estimate the effective active volume of typical GaInN/GaN MQW LEDs, we investigate a set of LED samples with different number of QWs. Figure 2(a) shows

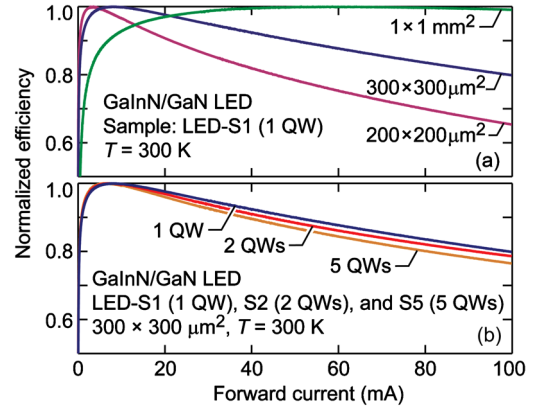


FIG. 2. (Color online) Normalized IQE as a function of current for GaInN/GaN LED samples (a) with different chip areas, and (b) with different number of quantum wells.

the normalized LED efficiency as a function of chip area for the single QW LED. The experimental result indicates that the current at peak efficiency increases with chip area as expected. Figure 2(b) shows the normalized efficiency as a function of current for $300 \times 300 \mu\text{m}^2$ LEDs with different number of QWs. The data, however, shows that current at peak efficiency does not strongly depend on number of QWs (the absolute-peak-intensity variation for these three samples is within $\pm 7\%$). This trend indicates that for typical MQW GaInN/GaN LED structures, the recombination occurs mainly in just one QW. Therefore, we take the volume of one QW as the effective active volume ($3 \text{ nm} \times 300 \mu\text{m} \times 300 \mu\text{m}$ for LED-1), and use this value to obtain $\eta_1 (=qV_{\text{active}})$.

Inserting $n_0 = \sqrt{A'/C'}$ into Eq. (2) yields

$$\frac{A'B'}{C'} = \frac{I_0 P}{\eta_1 (P+2)}, \quad (6)$$

where I_0 is the current at peak efficiency. Using Eq. (6) and $P=B'/\sqrt{A'C'}$ yields the following:

$$C' = B'^{3/2} \sqrt{\frac{1}{I_0} \frac{P+2}{\eta_1 P^3}} \quad (A' \text{ eliminated}), \quad (7)$$

$$C' = A'^3 (P+2)^2 (1/I_0)^2 \eta_1^2 \quad (B' \text{ eliminated}). \quad (8)$$

Given that low-density recombination is well described by SRH recombination, one can write $an \ll An$, or $A \approx A'$; in the general case, $f(n)$ may have 2nd, 3rd, and higher power terms. However, for highest-efficiency blue GaInN LEDs for which radiative recombination dominates in some current range (peak $\text{EQE} \gg 50\%$), one can write $\beta n^2 \ll Bn^2$, or $B \approx B'$. For LED-1, the values of I_0 , η_1 , and P are 0.42 mA, $4.3 \times 10^{-29} \text{ cm}^3 \text{ C}$, and 4.59, respectively. The B coefficient has been reported to be approximately $10^{-10} \text{ cm}^3 \text{ s}^{-1}$ (Refs. 2 and 10–13); therefore, the third-order non-radiative coefficient C' (or $C+\gamma$) is estimated from Eq. (7) and $B \approx B'$ to be about $8 \times 10^{-29} \text{ cm}^6 \text{ s}^{-1}$. This value is consistent with values of 10^{-29} – $10^{-27} \text{ cm}^6 \text{ s}^{-1}$ reported in the literature.^{10,14} However, much smaller Auger coefficients of 10^{-34} – $10^{-31} \text{ cm}^6 \text{ s}^{-1}$ have been reported based on first-principle theoretical calculations.^{15–17} Since no theory has predicted an Auger coefficient as large as $8 \times 10^{-29} \text{ cm}^6 \text{ s}^{-1}$ for GaInN/GaN LEDs and fitting procedures can in principle only give the total third-order coefficient without revealing

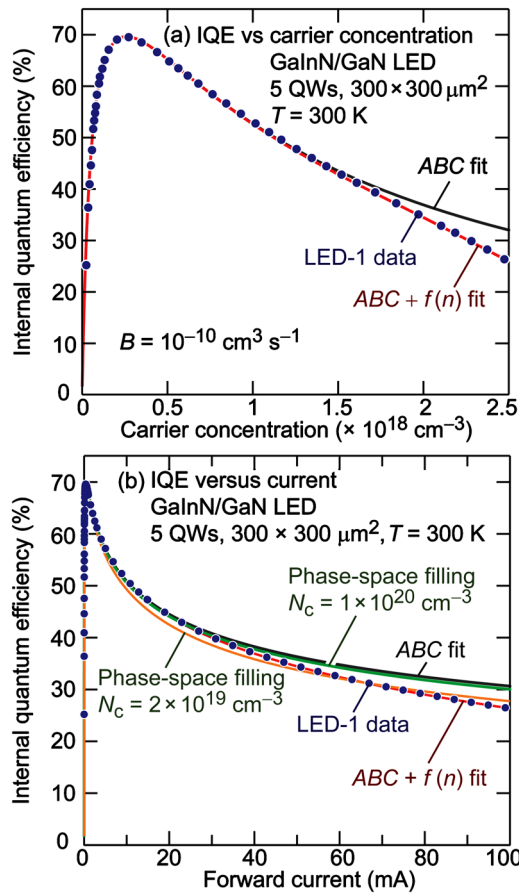


FIG. 3. (Color online) Internal quantum efficiency (a) vs carrier concentration, and (b) vs current, and theoretical fits using ABC model with phase-space filling adjustments and $ABC+f(n)$ model.

the specific contribution from leakage and Auger recombination, the discrepancy between the experimental third-order coefficient and the theoretical Auger coefficient may come from the γn^3 term, which is part of the leakage term $f(n)$.

Next, we investigate the LED-1 in greater detail: The peak internal quantum efficiency (IQE) is obtained by using Eqs. (4), (6), and $B \approx B'$, as follows:

$$IQE_{\max} = \frac{Bn_0^2}{G_0} = \frac{A'B/C'}{I_0/\eta_1} = \frac{A'B'/C'}{I_0/\eta_1} = \frac{P}{P+2}. \quad (9)$$

A peak IQE of 70% is obtained for LED-1 based on Eq. (9). Recalling the expression of y in Eq. (3b), it can be written as $y = \eta_2/\eta_1 \times IQE$. By inserting the value of η_1 , and the peak values y_0 and IQE_{\max} , one obtains the value of η_2 . By inserting η_2 into Eq. (2), Bn^2 is obtained. We obtain the carrier concentration n by assuming a B value of $10^{-10} \text{ cm}^3 \text{ s}^{-1}$.^{2,10-13} Figure 3(a) shows the IQE as a function of carrier concentration.

However, the function $f(n)$ will certainly depend on the design, structure, and doping of an LED. First, for lower-efficiency samples, the condition of $B \approx B'$ may not be fulfilled, revealing the possibility of a nonzero second-order term in $f(n)$; second, our analysis of the peak IQE of the sample LED-S5 indeed suggests that a considerable second-order term in $f(n)$ exists for this sample.

Finally, we analyze the possible effect of phase-space filling on the ABC model: The phase-space filling adjustment on the B coefficient has been modeled by using $B = B_0/(1 + n/N_C)$,^{10,12} where $B_0 = 10^{-10} \text{ cm}^3 \text{ s}^{-1}$.¹² Theoretical fitting

curves that take into account phase-space filling are shown in Fig. 3(b) for $N_C = 1 \times 10^{20}$ and $N_C = 2 \times 10^{19} \text{ cm}^{-3}$. Choosing these or other values of N_C and B_0 generally did not result in a good fit. Furthermore, taking into account phase-space filling for the C coefficient reduces the third-order non-radiative coefficient at high currents, which further increases the deviations of fit curves from experimental data. Therefore, the deviations may not be fully explained by the phase-space filling effect.

In summary, we model the carrier recombination in GaInN/GaN MQW LEDs as $R = An + Bn^2 + Cn^3 + f(n)$, and expand the leakage term $f(n)$ into a power series. We find that $f(n)$ has higher-than-third-order terms, which contribute about 14% to the total recombination rate at 111 A/cm^2 . The extracted total third-order nonradiative coefficient is $8 \times 10^{-29} \text{ cm}^6 \text{ s}^{-1}$. This large third-order coefficient determined by experiment and fitting could be explained by the term $f(n)$. Comparison of the theoretical $ABC+f(n)$ model with experimental data shows that a good fit requires the inclusion of the $f(n)$ term, particularly at high current densities.

Sandia authors and Q.D., Q.S., J.W., S.C., and J.C. were supported by Sandia's Solid-State Lighting Science Center, an Energy Frontier Research Center funded by the USDOE, Office of Science, Office of Basic Energy Sciences. Sandia is a multiprogram laboratory operated by Sandia Corporation, a wholly owned subsidiary of Lockheed Martin Co., for the USDOE's National Nuclear Security Administration under Contract No. DE-AC04-94AL85000.

¹M. H. Kim, M. F. Schubert, Q. Dai, J. K. Kim, E. F. Schubert, J. Piprek, and Y. Park, *Appl. Phys. Lett.* **91**, 183507 (2007).

²M. F. Schubert, S. Chhajed, J. K. Kim, E. F. Schubert, D. D. Koleske, M. H. Crawford, S. R. Lee, A. J. Fischer, G. Thaler, and M. A. Banas, *Appl. Phys. Lett.* **91**, 231114 (2007).

³J. Piprek, "Efficiency droop in nitride-based light-emitting diodes," *Phys. Status Solidi A* (to be published).

⁴M. F. Schubert, J. Xu, Q. Dai, F. W. Mont, J. K. Kim, and E. F. Schubert, *Appl. Phys. Lett.* **94**, 081114 (2009).

⁵M. F. Schubert, J. Xu, J. K. Kim, E. F. Schubert, M. H. Kim, S. Yoon, S. M. Lee, C. Sone, T. Sakong, and Y. Park, *Appl. Phys. Lett.* **93**, 041102 (2008).

⁶D. Zhu, A. N. Noemaun, M. F. Schubert, J. Cho, E. F. Schubert, M. H. Crawford, and D. D. Koleske, *Appl. Phys. Lett.* **96**, 121110 (2010).

⁷M. F. Schubert and E. F. Schubert, *Appl. Phys. Lett.* **96**, 131102 (2010).

⁸A. Y. Kim, W. Götz, D. A. Steigerwald, J. J. Wierer, N. F. Gardner, J. Sun, S. A. Stockman, P. S. Martin, M. R. Krames, R. S. Kern, and F. M. Steranka, *Phys. Status Solidi A* **188**, 15 (2001).

⁹Y. C. Shen, G. O. Mueller, S. Watanabe, N. F. Gardner, A. Munkholm, and M. R. Krames, *Appl. Phys. Lett.* **91**, 141101 (2007).

¹⁰A. David and M. J. Grundmann, *Appl. Phys. Lett.* **96**, 103504 (2010).

¹¹H. Y. Ryu, K. H. Ha, J. H. Chae, K. S. Kim, J. K. Son, O. H. Nam, Y. J. Park, and J. I. Shim, *Appl. Phys. Lett.* **89**, 171106 (2006).

¹²E. F. Schubert, *Light-Emitting Diodes*, 2nd ed. (Cambridge University Press, Cambridge, 2006).

¹³Q. Dai, M. F. Schubert, M. H. Kim, J. K. Kim, E. F. Schubert, D. D. Koleske, M. H. Crawford, S. R. Lee, A. J. Fischer, G. Thaler, and M. A. Banas, *Appl. Phys. Lett.* **94**, 111109 (2009).

¹⁴H.-Y. Ryu, H.-S. Kim, and J.-I. Shim, *Appl. Phys. Lett.* **95**, 081114 (2009).

¹⁵J. Hader, J. V. Moloney, B. Pasenow, S. W. Koch, M. Sabathil, N. Linder, and S. Lutgen, *Appl. Phys. Lett.* **92**, 261103 (2008).

¹⁶E. Kioupakis, P. Rinke, K. Delaney, A. Scheife, F. Bechstedt, and C. G. Van de Walle, *Proceedings of the Am. Phys. Soc. Meeting*, March 2010.

¹⁷J. Hader, J. V. Moloney, and S. W. Koch, *Appl. Phys. Lett.* **96**, 221106 (2010).